J. Fluid Mech. (2005), *vol.* 523, *pp.* 109–120.
DOI: 10.1017/S0022112004001971 Printed in the United Kingdom

Effect of absorption of solar radiation by water of different optical types on convection and heat transfer just under the air–water interface: the case of zero wind speed

By YU. G. VEREVOCHKIN[1] AND S. A. STARTSEV[2]

[1]Moscow State University for Geodesy and Cartography, Gorokhovskii 4, Moscow 105064, Russia
Verevochkin@yandex.ru

[2]Physical Lebedev Institute, Neutron Physics Department, Leninskii 53, Moscow 117924, Russia

(Received 14 November 2003 and in revised form 21 July 2004)

A horizontally infinite water layer cooled from above and absorbing solar radiation is considered. Optical water types are classified according to Jerlov (*Marine Optics*, Scientific, 1976). The convection and the heat transfer are simulated numerically based on the linear equation of state and the time-dependent two-dimensional heat-conduction and Navier–Stokes equations. To take into account the effect of solar radiation, the conventional heat-conduction law for water with a free surface is corrected by introducing a particular function of heat and solar-radiation fluxes. Analytical expressions for this function are fitted.

1. Introduction

An interfacial layer of water cooled from above and absorbing solar radiation is often divided into the cool skin and the warm layer. The former is characterized by a large temperature gradient, while the latter absorbs a considerable amount of incident solar energy. As a rule, these regions are considered separately based on different models. The cool skin has been investigated by Paulson & Simpson (1981), Soloviev & Schlüssel (1996), and Fairall *et al.* (1996), where the last group of investigators consider the warm layer as well. Paulson & Simpson (1981) examine the cool skin at zero and non-zero wind speed separately. They calculate the temperature drop across it based on formulae that are derived for radiation-free conditions and where heat flux through the free surface is reduced to take into account absorption of solar radiation. The absorption is characterized by nine attenuation lengths fitted for clear water. Fairall *et al.* (1996) treat the effect of solar radiation on the cool skin in a similar way, use the same parameterization of solar-radiation flux in water as Paulson & Simpson (1981), but modify the relations for the temperature drop across the cool skin by simultaneously taking into account both shear-driven and convectively driven turbulence.

Soloviev & Schlüssel (1996) consider the transformation of an undersurface sublayer with dominating molecular heat conduction into cool or warm skin under the assumption that heat flux through the interface is constant. They solve the heat-conduction equation in a motionless medium with heat release caused by absorption of solar radiation, with allowance for optical water types: for the first short-wave spectral band of nine bands considered by Paulson & Simpson (1981), the

irradiance-absorption coefficient is fitted for each optical water type. Soloviev & Schlüssel consider the initial temperature in the layer to be uniform and assume that the formation of a temperature profile in it is limited by a certain renewal time t_* at which the profile is completely destroyed by convection or long-wave breaking. Then, the cycle repeats itself.

The renewal time is dependent on wind speed, heat flux through the interface, downward irradiance, and the evaporation-caused increase in the near-surface salinity. The effect of the irradiance is to eliminate the term in t_* that describes the contribution of the surface cooling to it if a certain stability criterion is satisfied. However, this criterion, which was proposed by Woods (1980), is ill-founded because it is based on using the critical flux Rayleigh number corresponding to both no downward irradiance and a linear temperature profile. At zero wind speed, this ill-founded criterion dominates in the procedure of calculating the renewal time. Moreover, under this condition, the assumption that periodic destruction of the thermal sublayer is complete contradicts the calculations of Foster (1971) and Verevochkin & Startsev (2000) and the experimental data of Ginsburg, Zatsepin & Fedorov (1977). The renewal-type model discussed here excludes consideration of possible steady-state regimes of thermal convection.

The warm layer is considered by Woods (1980), Simpson & Dickey (1981), and Fairall *et al.* (1996). A part of the warm-layer analysis, which is carried out by Woods (1980) under the condition of light winds, is based on the above-mentioned ill-founded stability criterion. Simpson & Dickey (1981) consider the cases of both zero and non-zero wind speed based on the level-$2\frac{1}{2}$ version of the Mellor & Yamada (1974) turbulence closure scheme. As is known, in the case of zero wind speed, convection can be not only intermittent but also steady-state and cellular (see Foster 1971; Verevochkin & Startsev 1997, 2000). As the intermittent convection has, perhaps, some features of turbulence, the steady-state cellular convection can hardly be treated as turbulence. In addition, both versions of double-exponential parameterization used by Simpson & Dickey to model downward irradiance in water of different optical types are intended for water layers exceeding 10 m in depth. As will be shown below, near the interface, they describe weaker absorption of solar radiation than occurs in clear water characterized by the attenuation lengths proposed by Paulson & Simpson (1981). Fairall *et al.* (1996) consider warm-layer effects within the scope of a turbulent mixing model as well.

In contrast to the above-mentioned investigators, Verevochkin & Startsev (2000) do not divide a plane water layer into sublayers with *a priori* given properties. Under the condition of zero surface shear, they calculate temperature and velocity fields in the undersurface water by solving the heat-conduction and Navier–Stokes equations. It is the structure of the calculated temperature fields that allows an upper part of the water layer cooled from above and absorbing solar radiation to be treated as the cool skin. Regarding the sublayer adjacent to the bottom of the cool skin, turbulent behaviour is not imposed on it here. As a result, it turns out that, depending on the ratio of downward solar-radiation flux just under the interface to heat flux through the interface, the sublayer can be in a regime of intermittent convection, or in a regime of cellular steady-state convection, or convection-free. However, optical water types are not taken into account in this work. Moreover, it will be shown that parameterization of solar-radiation flux, which was proposed by Paulson & Simpson (1981) and used by Verevochkin & Startsev (2000) and Fairall *et al.* (1996), results in weaker absorption of solar energy by the undersurface clear water than occurs in reality. This aspect of the problem as well as a new parameterization of downward

irradiance, which takes into account the optical types of water and should be used within water layers some tens of centimetres thick, are discussed in the next section of this paper. This parameterization is used to investigate the effect of optical water types on processes occurring in the water just under the air–water interface at zero wind speed. These processes, in turn, determine the temperature drop across the cool skin, which represents a decrease in surface temperature with respect to the temperature maximum existing in water just below the interface (see Verevochkin & Startsev 2000). Temperature and velocity fields are calculated based on the model presented by Verevochkin & Startsev (2000). This model is free of empirical relations so that the results obtained are applicable for any basin filled with water of the corresponding optical type.

2. Parameterization of downward irradiance in water

Optical water types are classified according to Jerlov (1976), while the variation of downward solar-radiation flux with depth is modelled by the formula

$$J(z) = J_0 \sum_{i=1}^{9} D_i \exp(-z/\xi_i). \tag{1}$$

Here, J_0 is the downward solar-radiation flux in water just under the interface, z is the dimensional spatial coordinate taken vertically downward from the interface, D_i is the fraction of solar energy in each wavelength band, and ξ_i is the corresponding attenuation length. With one exception, we divide the solar-radiation spectrum into the same wavelength bands as Paulson & Simpson (1981). The exception is the first wavelength band, which ranges from 0.31 to 0.6 μm here and from 0.2 to 0.6 μm according to Paulson & Simpson (1981). Nevertheless, we use data of Paulson & Simpson (1981) for all D_i, because, according to Jerlov (1976), the fraction of incident solar radiation within the band 0.2–0.31 μm is negligible (see as well the spectral distribution of incident solar energy at the sea surface in Woods 1980, p. 382). Since the classification of Jerlov (1976) concerns the optical spectral range, we fit only ξ_1 and ξ_2 for each optical water type and take data of Paulson & Simpson (1981) for the last seven wavelength bands (the spectral range 0.9–3 μm). The details are as follows. When fitting ξ_1, we divide the wavelength band 0.31–0.6 μm into eleven subranges, where the first subrange is bounded by 0.31 and 0.35 μm, while the others are 0.025 μm wide. To each subrange, we assign the absorption coefficient K_i proposed by Jerlov (1976) for its lower boundary and calculate the function

$$J_\lambda(z) = \frac{\sum_{i=1}^{n} D_i' \exp(-K_i z)}{\sum_{i=1}^{n} D_i'}, \tag{2}$$

where the coefficients D_i' are proportional to fractions of incident solar energy in each subrange and $n = 11$. Then, function (2), which, for the considered spectral band, characterizes the attenuation of downward irradiance in water of a certain optical type, is approximated by the single exponential $\exp(-z/\xi_1)$ fitted within the 14 cm thick layer. The wavelength band 0.6–0.9 μm is divided into twelve 0.025 μm wide subranges. For the first five of them, K_i corresponding to a certain optical water type is taken from Jerlov (1976). For the others, we use the absorption coefficients

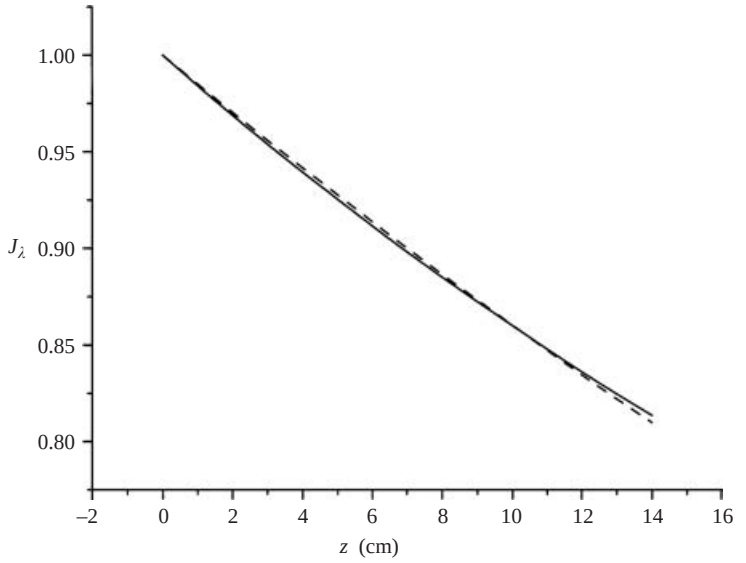

FIGURE 1. Function $J_\lambda(z)$ calculated for both optical water type II and the wavelength band 0.6–0.9 μm (solid line) and the fitted exponential $\exp(-z/\xi_2)$ (dashed line).

Water type	ξ_1 (m)	ξ_2 (m)
I	24.1	0.673
II	11	0.664
III	6.54	0.654
1	3.36	0.653
3	2.27	0.645
5	1.56	0.627
7	1.13	0.606
9	0.736	0.58

TABLE 1. Attenuation lengths fitted within the 14 cm thick layer for water of different optical types classified according to Jerlov in the spectral ranges 0.31–0.6 μm (ξ_1) and 0.6–0.9 μm (ξ_2).

presented by Curcio & Petty (1951) for distilled water. Then, the function $J_\lambda(z)$ in (2), where $n = 12$, is calculated and the exponential $\exp(-z/\xi_2)$ is fitted within the 14 cm thick layer. For the optical water type II, the function $J_\lambda(z)$ and the corresponding exponential $\exp(-z/\xi_2)$ are plotted in figure 1.

The attenuation lengths fitted in this way within 14 cm thick layers of water having different optical types are presented in table 1. Along with ξ_3–ξ_9 and D_i presented by Paulson & Simpson (1981), they are used to calculate curves (*d*) and (*e*) in figure 2, which compares the attenuation of downward irradiance according to different models. One can see that our calculation carried out for water of optical type I predicts much higher attenuation of downward irradiance than the parameterization of Simpson & Dickey (1981) and higher attenuation than even the parameterization of Paulson & Simpson (1981) developed for clear water. Since water of optical type I is almost clear, we considered the parameterization proposed by Paulson & Simpson (1981) more thoroughly. For this purpose, we fitted exponentials within layers of different thickness based on data of Defant (1961). These data show the spectral

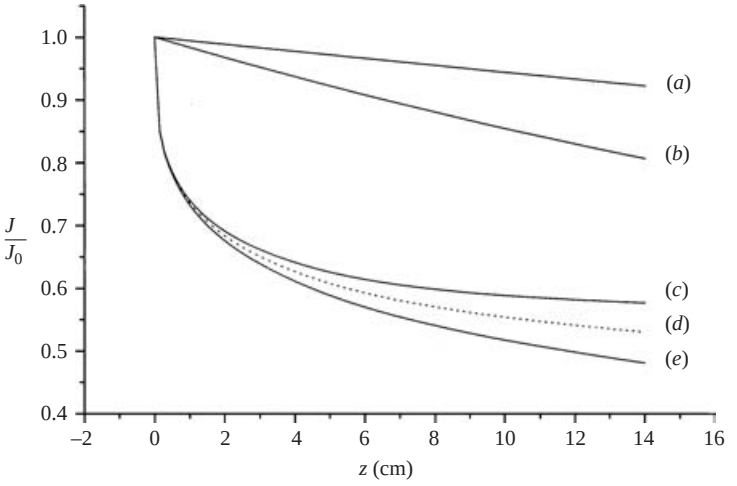

FIGURE 2. Vertical profiles of J/J_0 in water of different optical types: (*a*) type III (Simpson & Dickey 1981), (*b*) type I (Simpson & Dickey 1981), (*c*) clear water (Paulson & Simpson 1981), (*d*) type I (classification of Jerlov), (*e*) type 9 (classification of Jerlov). Here, J and J_0 are values of downward irradiance at depth z and just under the interface, respectively.

nine-band distributions of downward irradiance in water at certain depths and, in turn, were used by Paulson & Simpson (1981) to evaluate the attenuation lengths proposed by them. It turns out that the attenuation length ξ_1 equal to 34.8 m, which was proposed by Paulson & Simpson (1981) and used by Verevochkin & Startsev (2000) for the wavelength band 0.2 to 0.6 μm, corresponds to the fitting within the 100 m thick layer.

In the case of the 10 cm thick layer and the same wavelength band, ξ_1 fitted with the use of the two available points (see Defant 1961) is equal to 23.8 m. This value is close to the attenuation length ξ_1 obtained by us for both the spectral range 0.31–0.6 μm and water of optical type I according to the classification of Jerlov (see table 1). The attenuation length $\xi_2 = 2.27$ m, which was used by Paulson & Simpson (1981) and Verevochkin & Startsev (2000), corresponds to the 10 m thick layer. In the case of the 10 cm thick layer, the data of Defant (1961) yield $\xi_2 = 0.6$ m (see figure 3). This value is close to the attenuation lengths ξ_2 obtained by fitting exponentials within the 14 cm thick layer for water of all optical types (see table 1). The attenuation lengths ξ_3–ξ_9 used by Paulson & Simpson (1981) and Verevochkin & Startsev (2000) were fitted within layers less than 10 cm thick. Therefore, they are suitable for the problem under consideration, which concerns both modelling convection in water just under the air–water interface and calculation of the temperature drop across the cool skin. Note that the absorption coefficients obtained by Soloviev & Schlüssel (1996) for an unknown fitting depth and the first wavelength band do not lead to values of ξ_1 calculated here.

3. Modelling of temperature and velocity fields

We consider a plane horizontally infinite water layer cooled from above and absorbing solar radiation at zero wind speed. The layer has a free upper boundary and a rigid insulated bottom. The upward heat flux through the free boundary Q is

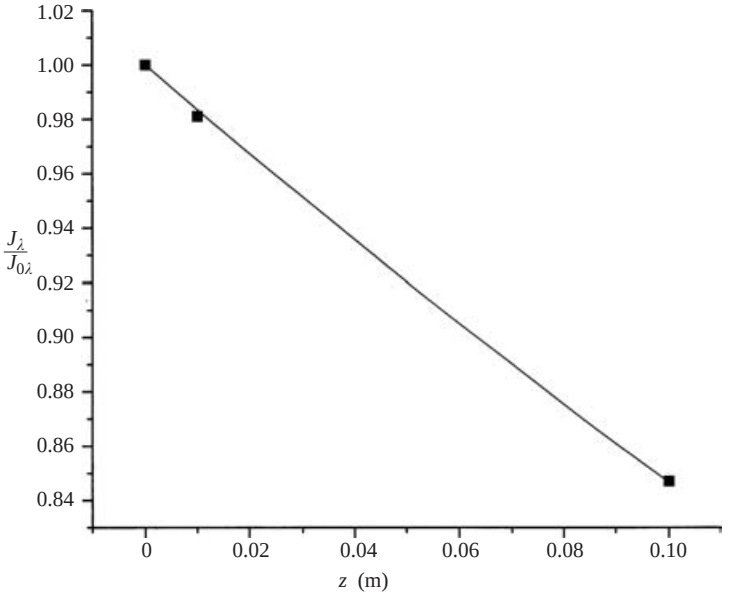

FIGURE 3. Ratio of downward irradiance at depth z (J_λ) to the irradiance just under water surface ($J_{0\lambda}$). Squares show data of Defant (1961) presented for the spectral band 0.6–0.9 μm and modelled by the exponential $\exp(-z/0.6)$ (line).

assumed to be time- and horizontal-coordinate-independent. The Prandtl number Pr is equal to 7. The mathematical model used here for solving the problem is discussed in detail by Verevochkin & Startsev (2000). Next, we recall some its features. Water is considered as an incompressible fluid with constant properties except for the density as it affects the buoyancy term (the Boussinesq approximation). The system of equations is formed by the linear equation of state, the time-dependent two-dimensional heat-conduction equation, and the time-dependent two-dimensional equation resulting from the Navier–Stokes equations. All equations are presented in dimensionless form, and solutions to them (temperature and velocity fields) are sought as Fourier series with spatial variables and time-dependent coefficients. These series are such that temperature and velocity necessarily satisfy specified boundary conditions. From this point of view, free boundary conditions are desirable for velocity, because they allow its vertical component to be sought as a sine series in the vertical spatial coordinate z and, in this way, simplify significantly the calculations.

However, free boundary conditions, which mean that no tangential force is applied to a fluid through its boundary, are not suitable for a free water surface. In fact, according to Berg, Acrivos & Boudart (1966), water can absorb surfactant substances, which reduce its surface tension. Therefore, if convective circulation broke the surfactant film, radially swept it out, and, in this way, increased the surface tension, it would undergo deceleration there. Due to this effect, a free water surface is never involved in gravity convection, which develops under it. So, Ginsburg *et al.* (1981), who used the shadow method to visualize gravity convection in fresh and salt water and in ethyl alcohol, write at the end of their paper that "Gravity convection developing in water does not affect the surface film... That is why a speck of dust, for hours, can be observed lying on a free surface of water in which turbulent convection has

developed." Since a free water surface is motionless it applies a tangential decelerating force to an underlying moving layer.

Using free boundary conditions in our model, we consider a free water surface as inelastic and replace the decelerating surface film by a decelerating sublayer, which is adjacent to the surface and where certain volume retarding forces are assumed to act. This replacement is obviously possible if the sublayer introduced is sufficiently thin. The necessary thinness is achieved by the method of fitting sublayer parameters: in a series of calculations, we increase the effectiveness of water deceleration in the sublayer (the parameter β_0 in (6), see Verevochkin & Startsev 2000) and decrease the sublayer thickness (the parameter $1/(2N_0)$ in (6), see Verevochkin & Startsev 2000) as long as the solution obtained varies. With these parameters fitted, the decelerating sublayer occupies a small upper part of the viscous sublayer and does not distort convective motion and heat transfer outside.

From the physical point of view, the effect of a motionless rigid boundary is identical to that of a motionless free water surface: they both decelerate adjacent water layers. Moreover, Ginsburg *et al.* (1981) present evidence that the type of boundary (rigid or free) is not important for gravity-convection heat transfer in water: temperature drops occurring in it near free and rigid boundaries are identical when identical heat fluxes are transferred through them. This would not be the case if the free surface moved. Motion of the free surface would intensify convective heat tranfer through it and, consequently, would decrease a temperature drop near it. This effect was observed, in particular, in ethyl alcohol, where, at identical tranferred heat fluxes, the temperature drop occurring near its free surface was approximately three times lower than near the rigid bottom (see Ginsburg *et al.* 1981). Allowing for the facts discussed above, we replace boundaries of both types by decelerating sublayers.

Earlier, we used our model to investigate convection and heat transfer in water filling vessels with insulated walls and bottom and cooled through its free surface in the absence of downward irradiance (Verevochkin & Startsev 1997). There are many experimental works that present reliable data concerning these phenomena under the above-mentioned conditions (see, for example, Katsaros *et al.* 1977), because it is easy to measure vertical temperature profiles in the laboratory environment and to calculate the heat flux through a free water surface, for example, by using the measured rate of water cooling. Therefore, the comparison of calculated and experimental data here can serve as an experimental verification of the model discussed. The mathematical model used in Verevochkin & Startsev (1997) is identical with that used in Verevochkin & Startsev (2000) under the condition that $J_0 = 0$.

The dimensionless system of equations forming the considered mathematical model at $J_0 = 0$ contains the Prandtl number Pr and the flux Rayleigh number $R = \alpha g Q h^4/(\nu\rho c k^2)$ as parameters. Here h is the layer thickness; k, the thermal diffusivity; ρ, water density at some reference temperature; c, the specific heat; α, the coefficient of thermal volume expansion; ν, the kinematic viscosity; and g, the acceleration due to gravity. If $R > 10^7$, convection is intermittent and, at any fixed spatial point, the water temperature varies with time almost as a random function. Our calculations (Verevochkin & Startsev 1997) were performed under this condition. Some instantaneous vertical temperature profiles are shown in figure 4. The cool skin is clearly seen there. However, this was not the subject of the investigation under discussion. The heat conduction law

$$Nu = ARa^n \tag{3}$$

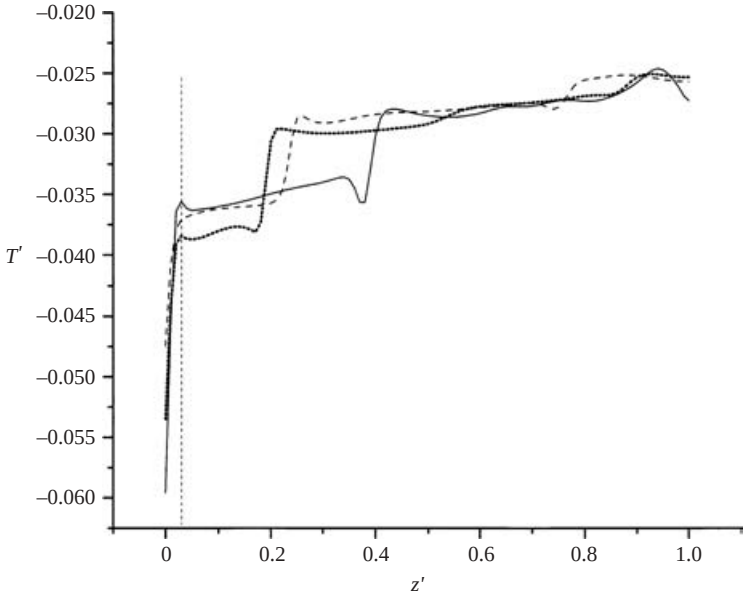

FIGURE 4. Instantaneous vertical profiles of dimensionless temperature at different moments of time, where z' is the dimensionless vertical coordinate normalized by the total layer thickness. The vertical dashed line ($z' = 0.034$) shows the average position of the cool-skin boundary for the profiles presented.

was under investigation there, where

$$Nu = \frac{QL}{\rho c k \Delta T} \tag{4}$$

is the Nusselt number and

$$Ra = \frac{\alpha g \Delta T L^3}{k\nu} \tag{5}$$

is the Rayleigh number. For water with a free surface, the empirical value of the constant A measured by different investigators varies from 0.11–0.13 (Grachev & Yaroshevich 1989) to 0.24–0.25 (Ginsburg & Fedorov 1978). In these experiments, ΔT was measured not as a time-average temperature drop across the cool skin but as an average temperature difference between the water surface and an undersurface level situated at a depth of about 10 cm (Grachev & Yaroshevich 1989) or 2 cm (Ginsburg & Fedorov 1978). Therefore, for different values of R and Pr, Verevochkin & Startsev (1997) calculated ΔT as the time-average temperature difference between the total-layer boundaries and considered the distance between these boundaries as a characteristic length L. In the case of room temperature, $Q = 100\ W/m^{-2}$, and for the considered range of R, this characteristic length varies from about 12 cm ($R = 5 \times 10^8$) to 17 cm ($R = 2 \times 10^9$). It turns out that the calculated ΔT satisfies the heat conduction law (3) with $n = 1/3$ and A not a constant but a function of the Prandtl number. For some values of the Prandtl number (some values of water temperature), the calculated values of A are shown in table 2. The calculated range of A covers more than a half of its range found experimentally. Unfortunately, quantitative comparison is possible only with the results of Katsaros *et al.* (1977), because only that paper presents data on water temperature during the experiments (21.6–42.7°C). The corresponding

T (°C)	Pr	A
40	4.3	0.144
20	7	0.16
5	11	0.21

TABLE 2. Dependence of the heat-exchange parameter A on the Prandtl number (water temperature).

calculated values of A are in the range 0.144–0.16, while the experimental value presented by Katsaros *et al.* (1977) is equal to 0.156. The remarkable agreement between these calculated and experimental data is obvious. In our opinion, this agreement proves experimentally that deceleration of water near both its free elastic surface and a rigid bottom can be modelled by using decelerating sublayers.

Now, let us turn to considering the effect of the optical water type on convection and heat transfer in the vicinity of the air–water interface. If the value of R is sufficiently large (water layer is sufficiently thick) then, near the interface, the dimensional solution to the problem is independent of the position of the layer bottom and, therefore, applicable for an arbitrarily deep water basin. Results of the calculations presented in this paper are obtained at $R = (1\text{–}5) \times 10^8$, corresponding to the above-mentioned condition.

Regardless of the specific optical water type, processes occurring under the interface are qualitatively the same as described by Verevochkin & Startsev (2000). They are characterized by the Rayleigh number (5), where, now, ΔT is the dimensional temperature drop across the cool skin or its time-average value if this quantity fluctuates, while L is a certain characteristic length, which has a different physical meaning in different regimes of convection. At small J_0/Q, the convection is intermittent and the temperature drop across the cool skin fluctuates. With increasing J_0/Q, the Rayleigh number, which is defined here by using the time-average depth of the undersurface temperature maximum z_m as a characteristic length ($L = z_m$), decreases. When it reaches its critical value Ra_{cr}, the convection becomes steady-state and ΔT jumps up. This transition occurs at $J_0/Q = 2.1$ in contrast to $J_0/Q = 1.9$ according to Verevochkin & Startsev (2000). The spatial scale of the steady-state mode of convection is equal to the thermal compensation depth, which, consequently, should be used as L when defining Ra. Note that, according to Woods (1980), the sublayer of thermal compensation absorbs solar radiation at a rate equal to the rate of surface energy loss. After a jump-like growth of Ra, which is associated with both change of the spatial scale of the convection and the jump of ΔT, an increase in J_0/Q causes a gradual decrease in both ΔT and Ra. When Ra reaches its critical value again, solar radiation quenches the convection without a jump of ΔT. Both the quenching of the convection and its transition to the steady-state mode occur at the same critical Rayleigh number $Ra_{cr} = 252\text{–}280$, which agrees with the calculations of Verevochkin & Startsev (2000). Temperature and velocity fields calculated here resemble qualitatively similar fields described by Verevochkin & Startsev (2000) and, therefore, are not presented in this paper. The time-average temperature drop across the cool skin ΔT calculated at different R satisfies a heat-conduction law of the form

$$Nu = ARa^{1/3} f(J_0/Q), \tag{6}$$

where $f(0) = 1$. Since Ra enters into (6) to a power of $\frac{1}{3}$, equations (4)–(6) yield the

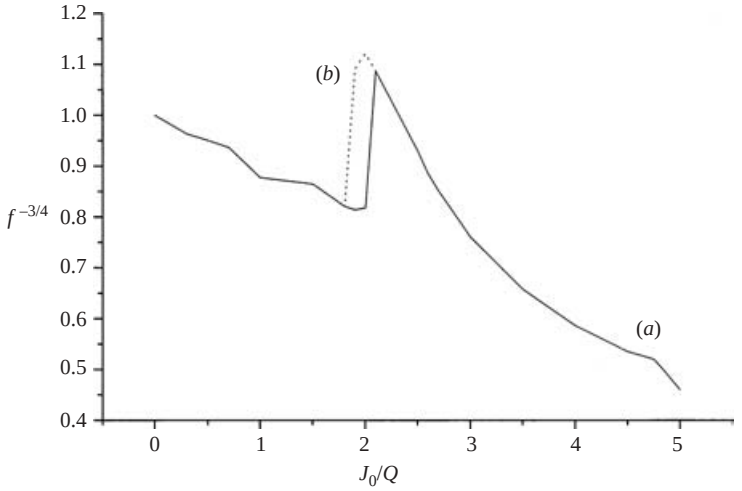

FIGURE 5. Function correcting the heat-conduction law to a power of $-\frac{3}{4}$ versus J_0/Q: solid line, this paper; dotted line, Verevochkin & Startsev (2000).

relation

$$\Delta T = A^{-3/4}\left(\frac{\nu}{\alpha g \rho^3 c^3 k^2}\right)^{1/4} Q^{3/4} f^{-3/4} \tag{7}$$

according to which ΔT is independent of L. Paulson & Simpson (1981) and Fairall *et al.* (1996) recommended use of a relation differing from (7) by the absence of the function $f^{-3/4}$ with $A = 0.2$ and $A = 0.23$, respectively. Our calculations carried out at $Pr = 7$, $J_0 = 0$ ($f = 1$), and different values of R yield $A = 0.215$. At $J_0 = 0$, the temperature drop across the cool skin is smaller than across the total water layer (see figure 4). Therefore, the value of the constant A calculated here is larger than that calculated by us for both the total water layer and the same value of the Prandtl number (see table 2). It is noteworthy that relations (6) and (7), *a priori*, are not imposed on the water layer, because we do not use them when calculating the temperature fields. Moreover, the governing dimensionless equations of our model even do not contain Nu and Ra as parameters (see Verevochkin & Startsev 2000). It is the form of the calculated temperature fields themselves that makes relations (6) and (7) valid. The function $f(J_0/Q)$, which enters (6) and (7), is identical for water of all optical types† and, to a power of $-\frac{3}{4}$, is shown in figure 5. At $J_0/Q \leqslant 1.8$ and $J_0/Q \geqslant 2.1$, it agrees with the calculations of Verevochkin & Startsev (2000). The range $1.8 < J_0/Q < 2.1$, where this agreement is violated, corresponds to the intermittent convection according to these calculations and to the steady-state convection according to Verevochkin & Startsev (2000). Thus, having been taken into account, the actual undersurface attenuation lengths of downward irradiance in oceanic water extend the region of existence of the intermittent convection from $J_0/Q \leqslant 1.8$ to $J_0/Q \leqslant 2$. We note that using $\xi_1 = 23.8$ m and $\xi_2 = 0.6$ m, which correspond to fitting exponentials for the data of Defant (1961) within the 10 cm thick layer, yields the same result. This extension is, probably, associated with the fact that an increase in absorption of solar radiation, which is associated with a decrease

† According to Soloviev & Schlüssel (1996), ΔT is practically independent of water type as well.

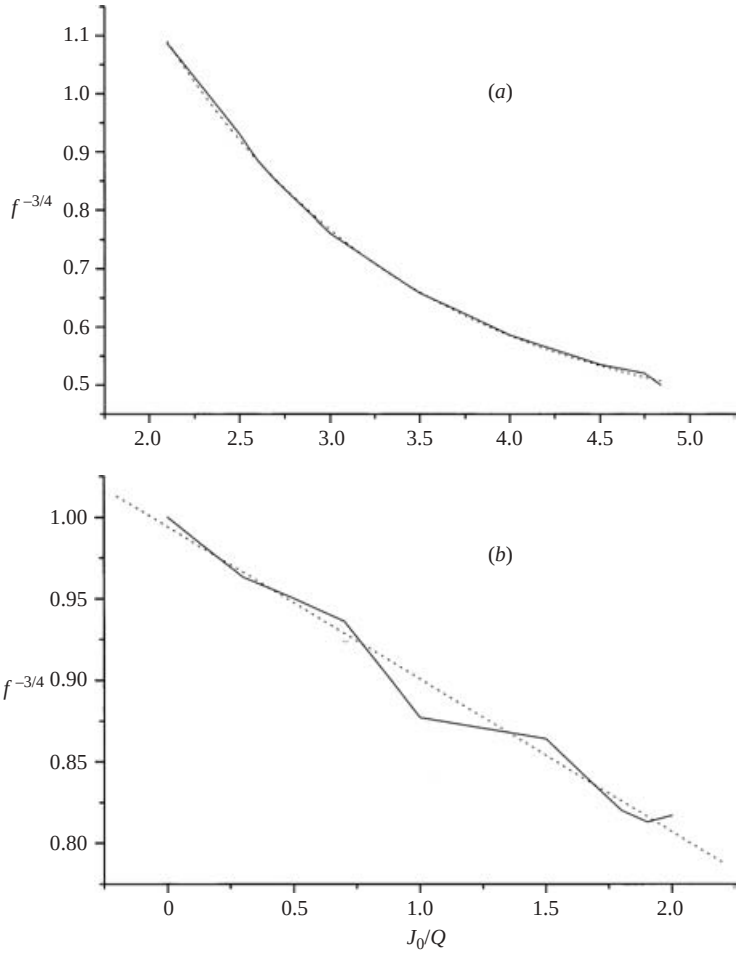

FIGURE 6. Numerical (solid line) and analytical (dotted line) representations of the function $f^{-3/4}(y)$ at (*a*) $4.8 \geqslant y \geqslant 2.1$ and (*b*) $y \leqslant 2$, where $y = J_0/Q$.

in attenuation lengths, diminishes the spatial scale of the steady-state convection (the thermal compensation depth) and, consequently, the corresponding Rayleigh number.

We have fitted analytical expressions for the function $f^{-3/4}(y)$ in the ranges $y \leqslant 2$ and $2.1 \leqslant y \leqslant 4.8$ ($y = J_0/Q$), which correspond to the regimes with convection:

$$f^{-3/4}(y) = y_0 + B \exp\left(-\frac{y}{t_0}\right) \quad \text{at} \quad 2.1 \leqslant y \leqslant 4.8, \tag{8}$$

$$f^{-3/4}(y) = P - Ty \quad \text{at} \quad y \leqslant 2, \tag{9}$$

where $y_0 = 0.41387$, $B = 3.08308$, $t_0 = 1.38337$, $P = 0.99412$, and $T = 0.09352$. Both these expressions and the numerically calculated function $f^{-3/4}(y)$ are plotted in figure 6.

Thus, taking into account the actual absorption of solar radiation by the undersurface water layer extends the range of the intermittent convection and changes the function $f(J_0/Q)$, which enters the heat-conduction law (6), (7) and, now, has an analytical representation.

REFERENCES

Berg, J. C., Acrivos, A. & Boudart, M. 1966 Evaporative convection. *Adv. Chem. Engng* **6**, 105.

Curcio, J. A. & Petty, C. C. 1951 The near infrared absorption spectrum of liquid water. *J. Opt. Soc. Am.* **41**(5), 302–304.

Defant, A. 1961 *Physical Oceanography*, vol. 1, p. 53. Pergamon.

Fairall, C. W., Bradley, E. F., Godfrey, J. S., Wick, G. A., Edson, J. B. & Young, G. S. 1996 Cool-skin and warm-layer effects on sea surface temperature. *J. Geophys. Res.* **101**(C1), 1295–1308.

Foster, T. D. 1971 Intermittent convection. *Geophys. Fluid Dyn.* **2**(3), 201–217.

Ginsburg, A. I., Dikarev, S. N., Zatsepin, A. G. & Fedorov, K. N. 1981 Phenomenological features of convection in liquids with a free surface. *Izv. Akad. Nauk SSSR, Fiz. Atmos. Okeana* **17**(4), 400–407.

Ginsburg, A. I. & Fedorov, K. N. 1978 Cooling of water from the surface under free and forced convection regimes. *Izv. Akad. Nauk SSSR, Fiz. Atmos. Okeana* **14**(1), 79–87.

Ginsburg, A. I., Zatsepin, A. G. & Fedorov, K. N. 1977 Fine structure of the thermal boundary layer forming in water near the air-water interface. *Izv. Akad. Nauk SSSR, Fiz. Atmos. Okeana* **13**(12), 1268–1276.

Grachev, A. A. & Yaroshevich, M. I. 1989 Measurements of free-convective heat transfer in water cooled from its free surface. *Izv. Akad. Nauk SSSR, Fiz. Atmos. Okeana* **25**(8), 887–890 (transl. *Izv. Acad. Sci. USSR, Atmos. Ocean. Phys.* **25**(8), 653 (1989)).

Jerlov, N. G. 1976 *Marine Optics*. Scientific Publishing Company, New York.

Katsaros, K. B., Lui, W. T., Businger, J. A. & Tillman, J. A. 1977 Heat transport and thermal structure in the interfacial boundary layer measured in an open tank of water in turbulent free convection. *J. Fluid Mech.* **83**, 311–335.

Mellor, G. L. & Yamada, T. 1974 A hierarchy of turbulence closure models for planetary boundary layers. *J. Atmos. Sci.* **31**, 1791–1806.

Paulson, C. A. & Simpson, J. J. 1981 The temperature difference across the cool skin of the Ocean. *J. Geophys. Res.* **86**(C11), 11044–11054.

Simpson, J. J. & Dickey, T. D. 1981 The relation between downward irradiance and upper ocean structure. *J. Phys. Oceanogr.* **11**, 309–323.

Soloviev, A. V. & Schlüssel, P. 1996 Evolution of cool skin and direct air-sea gas transfer coefficient during daytime. *Boundary-Layer Met.* **77**, 45–68.

Verevochkin, Yu. G. & Startsev, S. A. 1997 Use of decelerating sublayers in numerical simulation of gravity convection and heat transfer in a horizontal water layer. *Physica Scripta* **55**, 728–734.

Verevochkin, Yu. G. & Startsev, S. A. 2000 Numerical simulation of convection and heat transfer in water absorbing solar radiation. *J. Fluid Mech.* **421**, 293–305.

Woods, J. D. 1980 Diurnal and seasonal variation of convection in the wind-mixed layer of the ocean. *Q. J. R. Met. Soc.* **106**, 379–394.